

Local Elastic Constants in Thin Films of an FCC Crystal

Kevin Van Workum and Juan J. de Pablo

Department of Chemical Engineering, University of Wisconsin-Madison

In this work we present a formalism for the calculation of the local elastic constants in inhomogeneous systems based on a method of planes. Unlike previous work, this formalism does not require the partitioning of the system into a set of finite volumes over which average elastic constants are calculated. Results for the calculation of the local elastic constants of a nearest neighbor Lennard-Jones fcc crystal in the bulk and in a thin film are presented. The local constants are calculated at exact planes of the (001) face of the crystal. The average elastic constants of the bulk system are also computed and are consistent with the local constants. Additionally we present the local stress profiles in the thin film when a small uniaxial strain is applied. The resulting stress profile compares favorably with the stress profile predicted via the local elastic constants. The surface melting of a model for argon for which experimental and simulation data are available is also studied within the framework of this formalism.

PACS numbers: 68.08.-p, 68.35.Gy, 68.60.-p

I. INTRODUCTION

Knowledge of the local elastic constants in inhomogeneous systems is of significant theoretical, experimental, and industrial interest. As nanofabrication technologies improve and allow for the design and construction of nanoscopic devices, understanding the mechanical response of materials at nanometer length scales will become increasingly important. In particular, deviations from bulk, continuum behavior may lead to complications in the manufacturing of such devices. For example, in the microelectronics industry, the mechanical collapse of photoresist structures below 100nm may limit the ultimate density of memory storage devices or the performance of microprocessors [1, 2, 3].

In nanoscopic structures, interfaces are likely to play a major role in apparent deviations from bulk, continuum behavior [4]. The interface could either weaken or reinforce the overall mechanical behavior of the structure, depending on the nature of interactions between adjacent domains and the size of the structure. Understanding how mechanical properties vary near interfaces or free surfaces would provide insights into such phenomena.

Knowledge of interfacial behavior is crucial for understanding the adhesion of thin polymer films, where the inter-diffusion of the polymers and the molecular mobility near the film boundaries play a significant role [5]. Properties such as adhesion, dewetting, and surface melting in thin films are likely to be controlled by processes that occur within the first few nanometers of the interface. It would therefore be beneficial to have the ability to measure (computationally or experimentally) physical properties with molecular spatial resolution.

A microscopic definition for local elastic constants has been proposed in the literature [6, 7]. Implementation of that formalism requires that *layer-averaged* local elastic constants be determined. For inhomogeneous systems, the results from averaging over a particular layer depend strongly on the size and position of that layer. This is particularly true in an interfacial region or near a free sur-

face, where material properties can change significantly over short distances.

In this work, we are interested in the local elastic constants and surface melting of thin crystalline films. Specifically, we present a formalism in which the local elastic constants are calculated at precise planes in the system, as opposed to small volumes or slabs. In the bulk, the calculated local elastic constants are verified by averaging over the entire system and comparing the results to the bulk value. The local elastic constants in the film are verified by comparing the local stress profiles that arise from uniaxial strain and those calculated directly from the elastic constants.

II. THEORY

In a homogeneous material, applying a homogeneous strain necessarily results in a homogeneous stress. The stress is given by

$$\sigma_{ij} = C_{ijkl}\epsilon_{lk}, \quad (1)$$

where C_{ijkl} is the bulk elasticity tensor, and where the indices represent the cartesian coordinates in three dimensions.

When a homogeneous strain is applied to an inhomogeneous system, the resulting stress is also inhomogeneous. The local stress is then given by

$$\sigma_{ij}(\mathbf{r}) = C_{ijkl}(\mathbf{r})\epsilon_{lk}, \quad (2)$$

where $C_{ijkl}(\mathbf{r})$ is the *local* elasticity tensor. The relationship between the local and bulk elasticity tensors can be written as

$$C_{ijkl} = \frac{1}{V} \int_V C_{ijkl}(\mathbf{r}) d\mathbf{r}, \quad (3)$$

where V is the volume of the system.

The bulk elasticity tensor can be expressed in terms of the fluctuations of stress according to [8]

$$C_{ijkl} = 2\rho k_B T [\delta_{il}\delta_{jk} + \delta_{ik}\delta_{jl}] - \frac{V}{k_B T} [\langle P_{ij} P_{kl} \rangle - \langle P_{ij} \rangle \langle P_{kl} \rangle] + B_{ijkl}, \quad (4)$$

where ρ is the density, δ_{ij} is the Kronecker delta, P_{ij} is the pressure tensor and B_{ijkl} is the so-called Born term. The pressure tensor is given by

$$P_{ij} = \frac{1}{V} \left[\sum_a p_{a_i} p_{a_j} / m_a - \sum_{a < b} r_{ab}^{-1} u'_{ab} r_{ab_i} r_{ab_j} \right]. \quad (5)$$

The potential energy between interaction sites a and b is denoted by u_{ab} , r_{ab} is the distance between them, p_a and m_a are the momentum and mass of site a respectively, and the prime indicates a derivative with respect to r_{ab} . The Born term is related to the first and second derivatives of the potential energy of interaction by

$$B_{ijkl} = \frac{1}{V} \left\langle \sum_{a < b} \left[\frac{u''_{ab}}{r_{ab}^2} - \frac{u'_{ab}}{r_{ab}^3} \right] r_{ab_i} r_{ab_j} r_{ab_k} r_{ab_l} \right\rangle. \quad (6)$$

In this work we focus on the elastic properties of thin films having a planar symmetry; the films are assumed inhomogeneous only in the direction perpendicular to the film, i.e. z . Equation (4) must therefore be modified to calculate the elasticity tensor at precise planes within the system, without need for bins or small volumes. To this end, we use the method of planes (MOP) [9] and obtain an expression for the local elasticity tensor.

The first term in Eqn. (4) is the ideal gas contribution to the elasticity tensor. The kinetic energy is homogeneously distributed, even in inhomogeneous systems, and the temperature is independent of z . However, the density can vary in the z direction. The density profile, $\rho(z)$, could be calculated by dividing the system into many small bins and counting the average number of particles per unit volume in the bins. The density would then explicitly depend on the size of the bins used. Alternatively, one can use the fact that for a free standing film the total normal pressure, $P_{zz} = \rho(z)k_B T + P_{zz}^u(z)$, is constant throughout the system [10]. In vacuum, we then have for the density profile

$$\rho(z) = -\frac{P_{zz}^u(z)}{k_B T}, \quad (7)$$

where $P_{zz}^u(z)$ is the configurational contribution to the local pressure tensor. The local pressure tensor is the sum of ideal and configurational terms, and can be calculated according to [10, 11]

$$P_{ij}(z) = \rho(z)k_B T - \frac{1}{A} \left\langle \sum_{a < b} \frac{r_{ab_i} r_{ab_j}}{r_{ab}} u'(r_{ab}) \times \frac{1}{|z_{ab}|} \Theta\left(\frac{z - z_a}{z_{ab}}\right) \Theta\left(\frac{z_b - z}{z_{ab}}\right) \right\rangle, \quad (8)$$

where A is the cross-sectional area of the film and Θ is the Heaviside step function. The first term in Eqn. (4) can then be written for inhomogeneous systems as

$$C_{ijkl}^{id}(z) = 2\rho(z)k_B T [\delta_{il}\delta_{jk} + \delta_{ik}\delta_{jl}]. \quad (9)$$

The second term in Eqn. (4) arises from bulk stress fluctuations; it accounts for the non-zero temperature contribution to the elastic constants. We are interested in relating the local stress, $\sigma(z)$, to a bulk homogeneous strain. Therefore, instead of including the bulk-stress bulk-stress correlation, we use the correlation between the local-stress and the average bulk stress. The second term can then be written as

$$C_{ijkl}^{fluc}(z) = -\frac{V}{k_B T} [\langle P_{ij}(z) P_{kl} \rangle - \langle P_{ij}(z) \rangle \langle P_{kl} \rangle]. \quad (10)$$

Note that the volume V in Eqn. (10) cancels that in Eqn. (5) and there also is no explicit volume dependence in the MOP expression for $P_{ij}(z)$.

The Born term, Eqn. (4), can be calculated at planes using the MOP in the same way the local stress is determined, i.e. Eqn. (8). We have for the Born term in inhomogeneous systems

$$B_{ijkl}(z) = \frac{1}{A} \left\langle \sum_{a < b} \left[\frac{u''_{ab}}{r_{ab}^2} - \frac{u'_{ab}}{r_{ab}^3} \right] \frac{1}{|z_{ab}|} \Theta\left(\frac{z - z_a}{z_{ab}}\right) \times \Theta\left(\frac{z_b - z}{z_{ab}}\right) r_{ab_i} r_{ab_j} r_{ab_k} r_{ab_l} \right\rangle. \quad (11)$$

As before, this expression does not depend on the volume of the system or the (arbitrary) size of a bin.

The final expression for the local elasticity tensor in inhomogeneous systems with planar symmetry is given by

$$C_{ijkl}(z) = C_{ijkl}^{id}(z) + C_{ijkl}^{fluc}(z) + B_{ijkl}(z). \quad (12)$$

We emphasize again that this expression for $C_{ijkl}(z)$ is valid for inhomogeneous systems and is an average only over a cross section (a plane) of the system, not a discrete volume. It therefore relates the local stress (at z) to a homogeneous strain. Also note that Lutsko et al. [6] have presented a derivation for the local elasticity tensor, but they averaged over a sub-volume in order to facilitate the computations. It can be seen that by integrating over the entire system, one recovers the bulk elasticity tensor, Eqn. (4). We also note that this expression does not require the use of any dynamic variables but only requires ensemble averages taken from system configurations. It therefore is useful in either molecular dynamics or Monte Carlo (MC) simulations.

We note that other valid definitions of the local stress tensor have been presented [12, 13, 14] and discussed extensively in the literature [10, 15]. These definitions would in principle lead to different expressions for the local elasticity tensor. Regardless of the definition, one should expect to recover the bulk elasticity tensor after

averaging over the entire system. The definition used in this work is that of Irving and Kirkwood [11]. This definition was chosen here because it has been shown to be a physically valid stress tensor [15] and it can be used in MC simulations.

III. SIMULATIONS

To demonstrate the calculation of the local elasticity tensor, we employ the widely used nearest-neighbor Lennard-Jones (NNLJ) fcc crystal model [16, 17, 18, 19, 20, 21]. In what follows, all results will be reported in dimensionless Lennard-Jones units.

A bulk system consisting of 1000 particles with periodic boundary conditions in all three dimensions was investigated first. This system was simulated in the NVT ensemble at a temperature of $T = 0.3$ using a simple MC method. The density was chosen such that the average bulk pressure is zero. The center of mass of one atomic layer was held fixed at $z = 0$. The average bulk elastic constants for this system have been calculated previously and are listed in Table I. Reported elastic constants, stresses and strains are represented using Voigt notation [22]. For bulk fcc systems, there are three groups of non-zero, independent elements of the elastic constant matrix

$$C = \begin{bmatrix} C_{11} & C_{21} & C_{21} & 0 & 0 & 0 \\ C_{21} & C_{11} & C_{21} & 0 & 0 & 0 \\ C_{21} & C_{21} & C_{11} & 0 & 0 & 0 \\ 0 & 0 & 0 & C_{44} & 0 & 0 \\ 0 & 0 & 0 & 0 & C_{44} & 0 \\ 0 & 0 & 0 & 0 & 0 & C_{44} \end{bmatrix}. \quad (13)$$

Second, we also consider a free standing film of 450 particles. The free surfaces correspond to the (001) face of the fcc crystal. This system was also simulated in the canonical ensemble using a conventional MC method. In this case the cross sectional area was held constant with the same dimensions as the bulk system. The film had nine atomic layers parallel to the free surfaces. The temperature was the same as in the bulk, i.e. $T = 0.3$. The center of mass of the film was held fixed at $z = 0$. For an fcc film with free surfaces normal to the z -axis, there are six groups of non-zero, independent elements of the elastic constant matrix

$$C = \begin{bmatrix} C_{11} & C_{21} & C_{31} & 0 & 0 & 0 \\ C_{21} & C_{11} & C_{31} & 0 & 0 & 0 \\ C_{31} & C_{31} & C_{33} & 0 & 0 & 0 \\ 0 & 0 & 0 & C_{44} & 0 & 0 \\ 0 & 0 & 0 & 0 & C_{44} & 0 \\ 0 & 0 & 0 & 0 & 0 & C_{66} \end{bmatrix}. \quad (14)$$

Local properties of the film and the bulk system were calculated from Eqn. (12) at planes of constant z , with each plane being separated by a distance of 0.02 in both the thin film and bulk systems. The average elastic constants were also calculated in the bulk system from Eqn. (4).

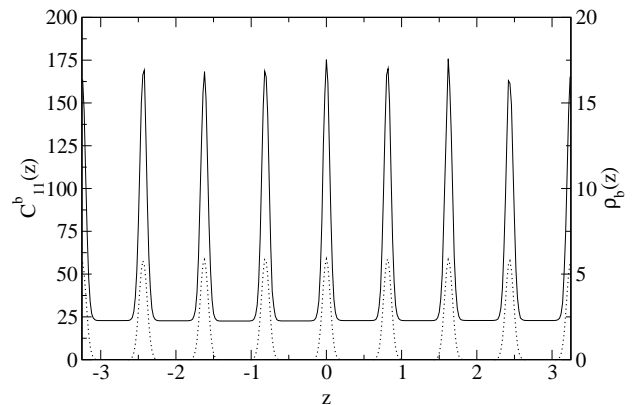


FIG. 1: $C_{11}^b(z)$ (solid line) as a function of z for the bulk system from Eqn. (12). The density profile, $\rho_b(z)$, is shown as the dotted line.

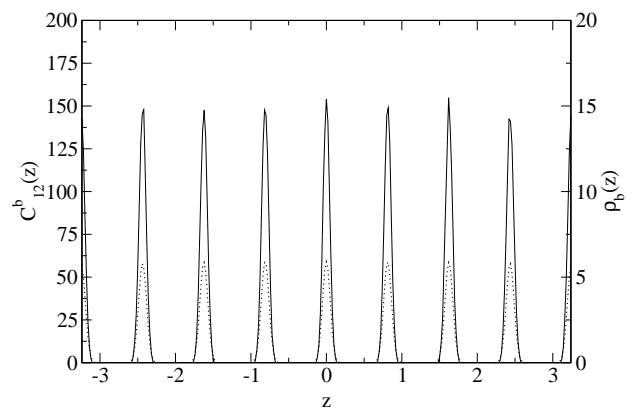


FIG. 2: $C_{21}^b(z)$ (solid line) as a function of z for the bulk system from Eqn. (12). The density profile, $\rho_b(z)$, is shown as the dotted line.

An additional simulation of the thin film was performed in which a homogeneous, tensile, uniaxial strain was applied in the x -direction, $\epsilon_1 = 0.01005$. The strain is defined as [23]

$$\epsilon_1 = \frac{1}{2} \left[\left(\frac{L_x}{L_x^0} \right)^2 - 1 \right], \quad (15)$$

where L_x is the length of the simulation cell in the x -direction, and L_x^0 is its original length. Since the strain is homogeneous, it is known that the average strain in a plane of atoms parallel to the free surface is equal to the applied strain [24]. The resulting stress profiles were then calculated using Eqn. (8). The stress profiles were also calculated directly from the elastic constants using Eqn. (2).

IV. RESULTS

The local elastic constant profiles for $C_{11}^b(z)$ and $C_{21}^b(z)$ in the bulk system are shown in Fig. 1 and Fig. 2 re-

C_{ij}	Ref [25]	Eqn. (4)	$Z^{-1} \int C_{ij}^b(z) dz$
C_{11}	43.35	43.22	43.37
C_{21}	19.01	19.45	19.22
C_{44}	22.50	22.60	22.35

TABLE I: Values of the three independent elastic constants of the bulk fcc crystal in dimensionless Lennard-Jones units. The last column is the average value of eight atomic layers of the (001) face in the bulk from Eqn. (12).

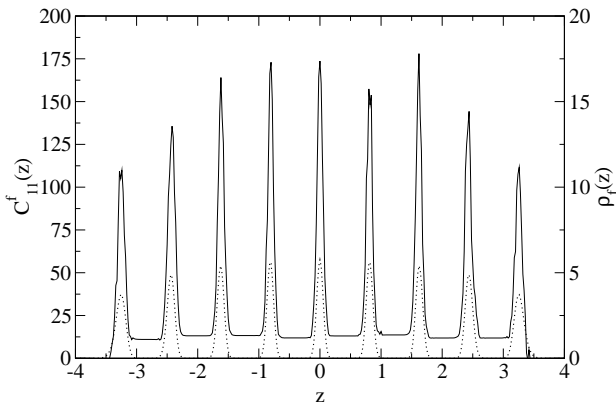


FIG. 3: $C_{11}^f(z)$ (solid line) as a function of z for the film system from Eqn. (12). The density profile, $\rho_f(z)$, is shown as the dotted line.

spectively. The density profile, $\rho_b(z)$, is also shown in these figures. Each peak in the profile at $C_{11}^b \approx 175$ and $C_{21}^b \approx 150$ corresponds to the center of mass of each atomic layer. Each minimum at $C_{11}^b \approx 22.5$ and $C_{21}^b \approx 0$ corresponds to the midpoint between each atomic layer. The local elastic constant profile for C_{44}^b is similar to C_{21}^b and is not shown.

The average bulk elastic constants can be calculated from the local constants using

$$C_{ij}^b = \frac{1}{Z} \int_Z C_{ij}^b(z) dz, \quad (16)$$

where Z is the width of the system. In this example, we set Z to the width of eight atomic layers in the bulk. The average bulk elastic constants calculated from Eqn. (16) are given in Table I. The bulk elastic constants from Eqn. (4) and the literature values [25] are also given in Table I. All three values for each elastic constant agree well with one another.

The local elastic constant profiles for $C_{11}^f(z)$ and $C_{21}^f(z)$ in the thin film are shown in Fig. 3 and Fig. 4, respectively. The density profile, $\rho_f(z)$, is also shown in these figures. The peaks corresponding to the atomic layers in the center of the film ($z = 0$) have approximately the same maximum values as in the bulk system, i.e. $C_{ij}^f(0) \approx C_{ij}^b(0)$. However, the minimum values between each layer near the center of the film are less than in the bulk. Interestingly, $C_{21}^f(z)$ exhibits negative values be-

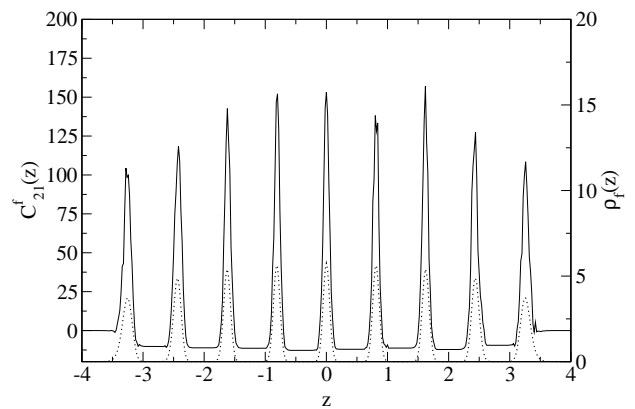


FIG. 4: $C_{21}^f(z)$ (solid line) as a function of z for the thin film from Eqn. (12). The density profile, $\rho_f(z)$, is shown as the dotted line.

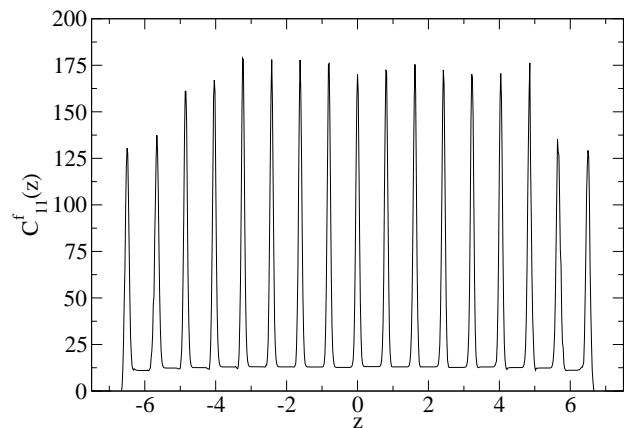


FIG. 5: $C_{11}^f(z)$ as a function of z for a film with 17 atomic layers.

tween each layer. The meaning of these negative values is discussed below.

The peak values of the elastic constants decrease from the center of the film as the free surfaces are approached. The profiles also become broader near the free surfaces. The decrease of the local elastic constants is an indication of the enhanced atomic mobility at the surfaces.

In order to investigate the effect of film thickness, a film consisting of 17 atomic layers was also simulated. Figure 5 shows the local elastic constant profile for $C_{11}^f(z)$ in the film with 17 layers. The effect of the free surface is limited to the first two atomic layers for both this system and that shown in Fig. 3. The elastic constant profiles for both film thicknesses are consistent with one another.

The local stress profiles are shown in Fig. 6 for $\sigma_1(z)$ and in Fig. 7 for $\sigma_2(z)$ after a homogeneous uniaxial strain was applied. The local stress profiles in the film were calculated from Eqn. (2) using the local elasticity tensor measured at zero strain. The local stress profiles were also calculated in the strained film as

$$\sigma_i(z) = -[P_i(z)|_{\epsilon=\epsilon_1} - P_i(z)|_{\epsilon=0}], \quad (17)$$

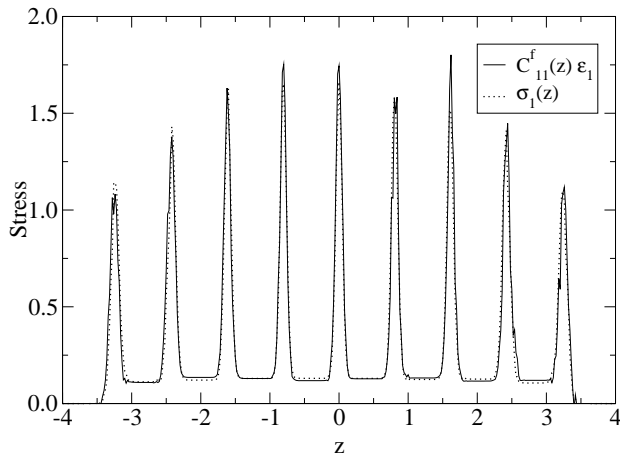


FIG. 6: Profiles for σ_1 in the thin film after a small homogeneous uniaxial strain, ϵ_1 , is applied. The solid line is calculated from the elastic constants and Eqn. (2), and the dotted line is calculated directly from the simulation using Eqn. (8).

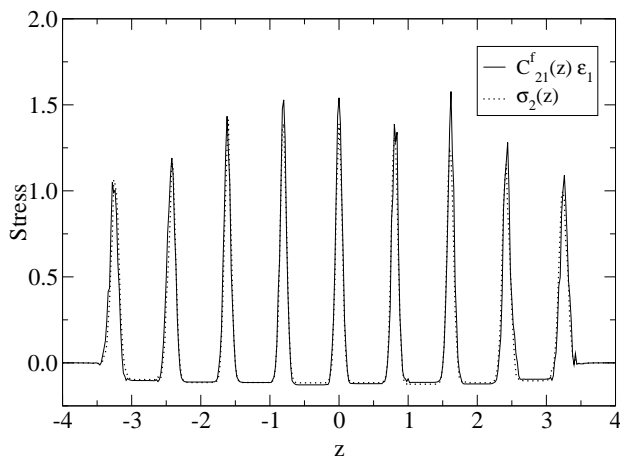


FIG. 7: Profiles for σ_2 in the thin film after a small homogeneous uniaxial strain, ϵ_1 , is applied. The solid line is calculated from the elastic constants and Eqn. (2), and the dotted line is calculated directly from the simulation using Eqn. (8).

where we used Eqn. (8) for $P_i(z)$. The results are shown in Fig. 6 and Fig. 7. The fact that the two methods for calculating the local stress profiles give the same result is reassuring and demonstrates that the response to the applied strain is linear. For $\sigma_2(z)$, we find that the tensile (positive) uniaxial strain in x -direction causes a negative stress in the region between the atomic layers (Fig. 7). This is directly related to the negative elastic constants seen in $C_{21}^f(z)$.

V. SURFACE MELTING

In order to study the melting behavior of a thin crystalline film, we adopt the model for argon used by Eerden et al. [26]. As before, we study the (001) surface of the

crystal. The interaction is described by the truncated LJ potential given by

$$u_{ab} = 4.569\epsilon \left[\left(\frac{r_{ab}}{\sigma} \right)^{-12} - \left(\frac{r_{ab}}{\sigma} \right)^{-6} \right] \times \exp \left(\frac{0.25\sigma}{r_{ab} - 2.5\sigma} \right). \quad (18)$$

Eerden et al. report the bulk elastic properties for this system.

Consistent with Eerden et al., we have 32 atoms in each layer of the crystal and use films consisting of 16 layers. The elastic constants are calculated at planes in the top half of the film separated by a distance of $dz = 0.02$. At each temperature, the lateral dimensions of the simulation cell were taken from the average size of a bulk simulation cell at zero pressure. The surface of the film was aligned perpendicular to the z -axis and the center of mass was fixed at $z = 0$.

Analogous to the definition of the average lateral shear modulus for a slab between z and z' ($\mu^\sigma[z, z']$) by Eerden et al., we define the local lateral shear modulus at a plane z as

$$\mu_i^\sigma(z) = \frac{1}{8} \sum_{\alpha=x,y} \sum_{\beta=x,y} [C_{\alpha\beta\beta\alpha}(z) + C_{\alpha\beta\alpha\beta}(z) - C_{\alpha\alpha\beta\beta}(z)]. \quad (19)$$

Note that this definition is a projected (onto the xy -plane) version of the usual shear modulus for an isotropic solid [7]. Since we are interested in the melting behavior of an anisotropic solid, another useful definition of the local lateral shear modulus is

$$\mu_a^\sigma(z) = C_{66}(z). \quad (20)$$

As the crystal nears its melting point it becomes less anisotropic and we expect μ_a^σ to approach μ_i^σ . The melting point is defined here as the temperature at which μ_a^σ and μ_i^σ vanish.

The shear moduli as a function of position in the film are shown in Fig. 8 at four different temperatures. The density profiles at these temperatures are shown in Fig. 9. The density profile has units of σ^{-3} and its integral over the entire system, $A \int_z \rho(z) dz$, gives the total number of particles in the film. In the following discussion, we will refer to the layers starting with the surface layer as layer-1, layer-2, etc.

The behavior at the lowest temperature (Fig. 8a.), $T = 0.4$, is similar to that of the NNLJ film, having bulk behavior in the center of the film and decreasing moduli in the layers near the surface. The difference between μ_i^σ and μ_a^σ reflects the fact that the crystal is anisotropic, even in the layer nearest to the surface, layer-1. This is also evident in the density profile (Fig. 9a.) where all the atomic layers of the crystal are separated by regions of empty space. At temperatures above $T = 0.4$, isolated atoms have sufficient energy to escape layer-1 and occupy

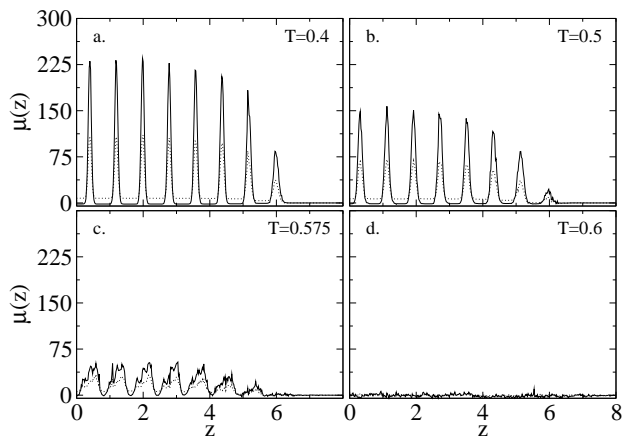


FIG. 8: The shear moduli profiles in a thin film of argon at four temperatures. The solid line is the μ_a^σ and the dotted line is μ_i^σ .

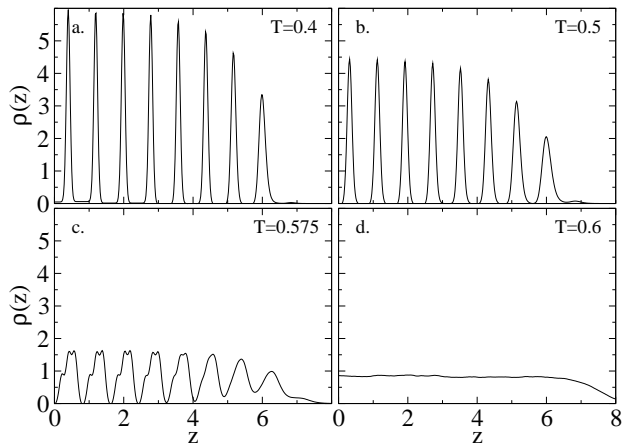


FIG. 9: The density profiles in a thin film of argon at four temperatures.

positions outside the film (layer-0). This additional layer can be seen as the very small peak centered at $z = 6.82$. The additional layer, however, has a zero shear modulus.

At $T = 0.5$, the shear moduli (Fig. 8b.) of each layer have decreased from those at $T = 0.4$, indicating a softening of the crystal. The difference between μ_i^σ and μ_a^σ has decreased considerably in layer-1, indicating nearly isotropic behavior near the melting temperature. The number of atoms which escape from layer-1 has increased, indicated by the larger peak or shoulder in the density profile (Fig. 9b.) at $z = 6.82$.

In Fig. 8c. and Fig. 9c. ($T = 0.575$), the behavior of the layers near the surface has changed significantly. Both μ_i^σ and μ_a^σ are essentially zero (indicating isotropy and melting) at layer-1 even though the density profile exhibits some remaining structure in that region. Between layer-1 and layer-2 and between layer-2 and layer-3, the density is non-zero yet the shear modulus is zero. A small amount of argon exists as a fluid between these layers. Layer-0 contains even more atoms at this tem-

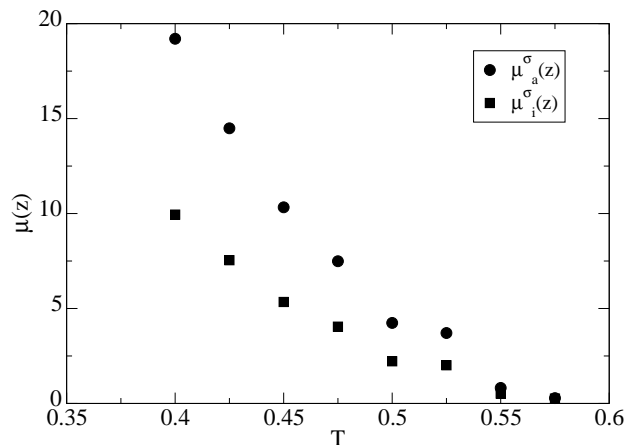


FIG. 10: The average lateral shear moduli in a thin argon film as a function of temperature.

perature and shows a flat density shoulder which decays to zero, indicating a loss of structure at the film-vacuum interface. At temperatures just below $T = 0.575$ and above, the delineation of layer thickness becomes ambiguous and the use of a layer-averaged shear modulus becomes questionable. The method of planes proposed here eliminates that ambiguity.

At $T = 0.6$, the shear modulus of the entire film is zero and the density profile is flat. The film is a liquid throughout and has none of the structure originally present in the crystalline film at lower temperatures.

An average shear modulus for the surface layer can be defined by integrating the profiles in Fig. 8. The average shear modulus is given by

$$\bar{\mu}^\sigma = \frac{1}{\Delta z} \int_{z_{\min}}^{z_{\max}} \mu^\sigma(z) dz. \quad (21)$$

A layer thickness Δz must first be defined in order to perform the integration. We arbitrarily choose Δz for the surface layer to be the distance between the peaks in the density profile of layer-1 and layer-2 at each temperature. In Eqn. (21), z_{\min} is the location of the minimum density between layer-1 and layer-2 and $z_{\max} = z_{\min} + \Delta z$.

The results for $\bar{\mu}_i^\sigma$ and $\bar{\mu}_a^\sigma$ of the surface layer are shown in Fig. 10 for temperatures up to $T = 0.575$. Both shear moduli decrease sharply with increasing temperature and vanish at $T = 0.575$, indicating melting of the surface layer. This is in agreement with the literature value of $T = 0.576$. The bulk melting temperature is $T_b = 0.601$ [26].

VI. CONCLUSION

A formalism for calculation of the local elastic constants in inhomogeneous systems based on the method of planes has been presented. Unlike previous work, this formalism does not require the partitioning of the system

into a set of finite volumes or “slabs” over which average elastic constants are calculated. As an example application of the technique, Monte Carlo simulations of the nearest-neighbor Lennard-Jones fcc crystal in the bulk and in thin film geometries have been presented.

The local atomic structure of the crystals was evident in the local elastic constants calculated at precise planes. In the thin film, the elastic constants are decreased from the corresponding bulk values, especially near the free surfaces. This decrease near a free surface is expected

to give rise to apparent deviations from bulk continuum behavior in thin films and nanoscopic structures.

The melting behavior of argon in a thin film was also investigated within the context of this formalism. Results show how the shear modulus profile of the surface layer of atoms vanishes below the melting temperature of the core of the film. Below the melting temperature of the film, the free surface allows sufficient thermal motion for the surface atoms to reach an isotropic liquid state prior to the bulk of the film.

-
- [1] T. Tanaka, M. Morigami, and N. Atoda, *Jpn. J. Appl. Phys.* **32**, 6059 (1993).
- [2] H. Cao, P. Nealey, and W. Domke, *J. Vac. Sci. & Tech. B* **18**, 3303 (2000).
- [3] T. Boehme and J. de Pablo, *J. Chem. Phys.* **116**, 9939 (2002).
- [4] D. Fryer, R. Peters, E. Kim, J. Tomaszewski, J. J. de Pablo, P. Nealey, C. White, and W. Wu, *Macromolecules* **34**, 5627 (2001).
- [5] J. A. Torres, P. F. Nealey, and J. J. de Pablo, *Phys. Rev. Lett.* **85**, 3221 (2000).
- [6] J. Lutsko, *J. Appl. Phys.* **64**, 1152 (1988).
- [7] J. van der Eerden, A. Roos, and J. van der Veer, *J. Crystal Growth* **99**, 77 (1990).
- [8] J. R. Ray, *J. Appl. Phys.* **53**, 6441 (1982).
- [9] B. D. Todd, D. J. Evans, and P. J. Davis, *Phys. Rev. E* **52**, 1627 (1995).
- [10] F. Varnik, J. Baschnagel, and K. Binder, *J. Chem. Phys.* **113**, 4444 (2000).
- [11] J. H. Irving and J. G. Kirkwood, *J. Chem. Phys.* **18**, 817 (1950).
- [12] D. Tsai, *J. Chem. Phys.* **70**, 1275 (1979).
- [13] J. Rowlinson and B. Widom, *Molecular Theory of Capillarity* (Oxford, 1982).
- [14] A. Harasima, *Adv. Chem. Phys.* (1958).
- [15] B. Hafskjold and T. Ikeshoji, *Phys. Rev. E* **66**, 011203 (2002).
- [16] M. Parrinello and A. Rahman, *J. Appl. Phys.* **52**, 7182 (1981).
- [17] P. J. Fay and J. R. Ray, *Phys. Rev. A* **46**, 4645 (1992).
- [18] M. Sprik, R. W. Impey, and M. L. Klein, *Phys. Rev. B* **29**, 4368 (1984).
- [19] E. R. Cowley, *Phys. Rev. B* **28**, 3160 (1983).
- [20] M. Li and W. L. Johnson, *Phys. Rev. B* **46**, 5237 (1992).
- [21] J. R. Ray, M. C. Moody, and A. Rahman, *Phys. Rev. B* **32**, 733 (1985).
- [22] J. F. Nye, *Physical Properties of Crystals: Their Representation by Tensors and Matrices* (Clarendon Press, Oxford University Press, 1984).
- [23] A. E. H. Love, *A Treatise on the Mathematical Theory of Elasticity* (Cambridge Univ. Press., 1927), 4th ed.
- [24] M. Kluge, D. Wolf, J. Lutsko, and S. Phillpot, *J. Appl. Phys.* **67**, 2370 (1990).
- [25] A. A. Gusev, M. M. Zehnder, and U. W. Suter, *Phys. Rev. B* **54**, 1 (1996).
- [26] J. P. v.d. Eerden, H. J. F. Knops, and A. Roos, *J. Chem. Phys.* **96**, 714 (1992).